J. Astrophys. Astr. (2008) **29,** 239–242

Numerical Simulations of Kinetic Alfvén Waves to Study Spectral Index in Solar Wind Turbulence and Particle Heating

R. P. Sharma* & H. D. Singh
Center for Energy Studies, Indian Institute of Technology, Delhi 110 016, India.
**e-mail: rpsharma@ces.iitd.ernet.in*

Abstract. We present numerical simulations of the modified nonlinear Schrödinger equation satisfied by kinetic Alfvén waves (KAWs) leading to the formation of magnetic filaments at different times. The relevance of these filamentary structures to solar wind turbulence and particle heating has also been pointed out.

Key words. Kinetic Alfvén wave: filamentation—solar wind—spectral index—chaotic structure.

1. Introduction

Alfvén wave turbulence is commonly observed in space plasmas, especially in the solar wind, the magnetosheath and auroral regions. The kinetic Alfvén wave (KAW) is obtained when the magnetohydrodynamic (MHD) Alfvén wave develops a large wavenumber, $k_\perp$, transverse to the ambient magnetic field B_0. The KAW carries nonzero parallel electric and magnetic field perturbations which contribute to plasma energization and particle acceleration. One such means for transferring energy from the large scale to small scale is the transverse collapse leading to the formation of strong magnetic filaments parallel to the ambient field, as asymptotically predicted by the nonlinear Schrödinger equation for the wave envelope (Champeaux *et al.* 1997, 1998; Laveder *et al.* 2001, 2002).

The motivation of this article is to solve the modified nonlinear Schrödinger equation (MNLSE) satisfied by the KAW numerically and study the transient filamentation process arising on account of the coupling between the main KAW and the perturbation.

2. Model equations

The dynamical equation governing the propagation (in the x–z plane) of low frequency, long wavelength, and finite amplitude KAW (magnetized by a uniform ambient magnetic field B_0 along the z direction), for intermediate plasma beta ($m_e/m_i < \beta < 1$; $\beta = 8\pi n_0 T/B_0^2 < m_e/m_i$) is governed by the MNLS equation (Bellan & Stasiewicz 1998; Shukla & Stenflo 1999, 2000; Shukla *et al.* 1999; Shukla & Sharma 2002) in dimensionless form,

$$i\frac{\partial B_y}{\partial t} + i\frac{\partial B_y}{\partial z} + 2i\Gamma\frac{\partial B_y}{\partial x} + \frac{\partial^2 B_y}{\partial x^2} + |B_y|^2 B_y = 0, \tag{1}$$

where $\partial_z B_y \ll k_{0z} B_y$, $m_e(m_i)$ is the mass of the electron (ion), n_0 is the unperturbed plasma number density, $T(= T_e \approx T_i)$ is the plasma temperature. $\Gamma = (v_{te}/v_A)k_{0x}\lambda_e$ is a parameter characterizing the normalized perpendicular wave number in terms of electron's collisionless skin depth, $v_{te}(= \sqrt{T_e/m_e})$ is the electron thermal speed, $v_A(= \sqrt{B_0^2/4\pi n_0 m_i})$ is the Alfvén speed, $k_{0x}(k_{0z})$ is the component of the wave vector perpendicular (parallel) to $\hat{\mathbf{z}}B_0$, and $\lambda_e(= \sqrt{c^2 m_e/4\pi n_0^2})$ is the collisionless electron skin depth. The normalizing values are $t_n = (2\omega/v_A^2 k_{0z}^2)(1 + k_{0x}^2\lambda_e^2)$, $z_n = 2/k_{0z}$, $x_n = v_{te}\lambda_e/v_A$, and $B_n = [\{1 - \Delta(1 + \delta)\}v_A^2 k_{0z}^2/16\pi n_0 T_e \omega^2]^{-1/2}$ where ω is the Alfvén wave frequency, $\Delta = \omega^2/\omega_{ci}^2$, $\delta = m_e k_{0x}^2/m_i k_{0z}^2$, and $\omega_{ci}(= cB_0/m_i c)$ is the ion gyrofrequency.

3. Numerical simulations

We have carried out 2D pseudospectral simulation of equation (1) numerically in a $(2\pi/\alpha_x) \times (2\pi/\alpha_z)$ periodic domain with $\alpha_x, \alpha_z = 1$ and $(128)^2$ grid points with initial condition of simulation

$$B_y(x, z, 0) = |B_{y0}|(1 + 0.1\cos(\alpha_x x))(1 + 0.1\cos(\alpha_z z)), \tag{2}$$

where B_{y0} is the amplitude of the homogenous pump KAW. The finite difference with predictor–corrector method was used for the integration of time with a small time step of $dt = 5 \times 10^{-4}$. The results of filament formation of KAW for various times and keeping $\Gamma(= 0.01)$ fixed are presented below.

The time evolution of the intensity of the transverse magnetic field is exemplified in Fig. 1(a–d) by means of snapshots at four instants of time ($t = 1.5, 2, 2.5, 4.5$). It is evident from the figure that at early times more intense filaments are formed and with the advancement of time, these become chaotic structures. Once the chaotic structure is formed, the filaments become more or less chaotic at later times.

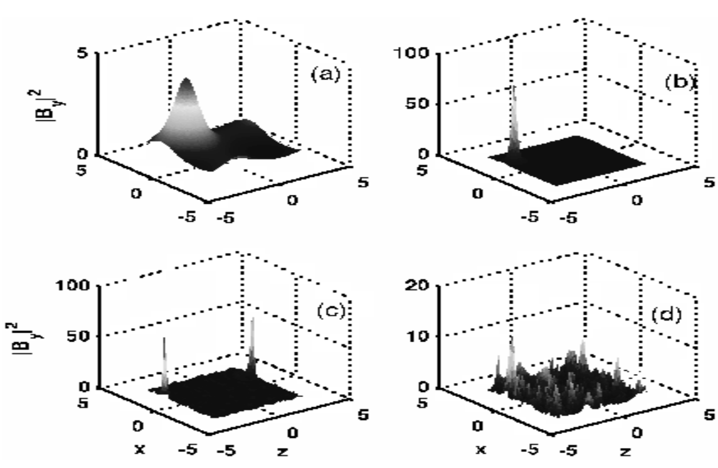

Figure 1. The magnetic-field intensity profiles of KAW. **(a)** $t = 1.5$, **(b)** $t = 2$, **(c)** $t = 2.5$, and **(d)** $t = 4.5$.

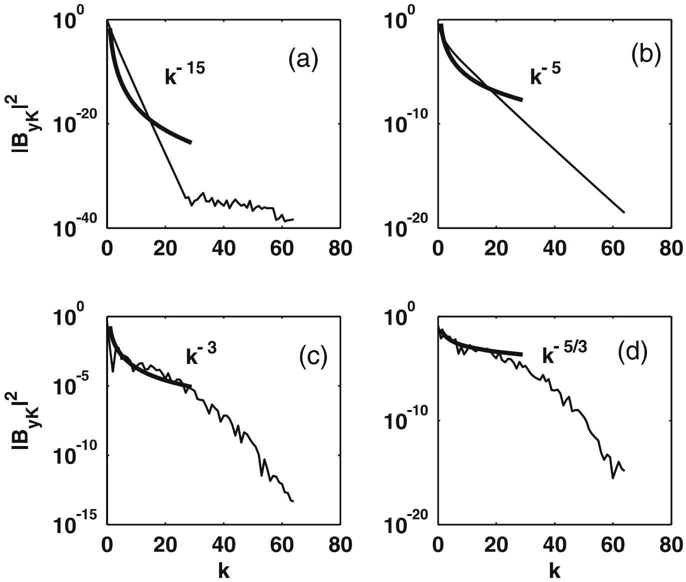

Figure 2. Variation of $|B_{yk}|^2$ against k_z at $k_x = 0$ for KAW. **(a)** $t = 1.5$, **(b)** $t = 2$, **(c)** $t = 2.5$, and **(d)** $t = 4.5$. The thick line curve indicates the spectral index scaling.

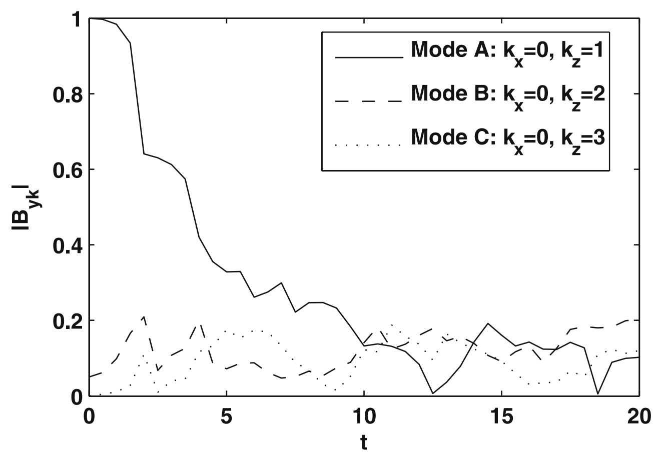

Figure 3. Time evolution of $|B_{yk}|$ of three Fourier modes for KAW.

Figure 2(a–d) shows the variation of $|B_k|^2$ against k_z for a fixed value of $k_x = 0$ at different times. It is evident from the wavenumber spectrum that the spectral index is steeper than the Kolmogorov $k^{-5/3}$ scaling at early times. But as time advances, it approaches Kolmogorov $k^{-5/3}$ scaling. This is in agreement with the power spectra for various time series found by Goldstein *et al.* (1999) that for late time and large distances, the spectral index approached Kolmogorov $k^{-5/3}$ scaling.

Figure 3 shows the time evolution of the amplitudes of several wave modes and represents that the nonlinear growth of the mode A occurs at $t = 12.5$. Since the $k^{-5/3}$

scaling has already formed at $t = 4.5$, the growth of the mode A at $t = 12.5$ occurred under the turbulent state of waves. Modes B and C grow first and decay showing the oscillatory evolution.

For application purposes, the typical values of several solar wind parameters as measured by Helios 2 at 1 AU are $B_0 \approx 6\,\text{nT}$, $n_0 \approx 3\,\text{cm}^{-3}$, $T \approx 10\,\text{ev}$; then $\beta \approx 0.335$, $v_A \approx 7.7 \times 10^6\,\text{cm/s}$, $v_{te} \approx 1.3 \times 10^8\,\text{cm/s}$, $\omega_{ci} \approx 0.6\,\text{Hz}$, and $\rho_s \approx 5.3 \times 10^6\,\text{cm}$. For these typical parameters at $\omega/\omega_{ci} = 0.02$ and $k_x\rho_s = 0.01$, the magnitudes of the fluctuations are $|\delta B_{y0}|/B_0 = 0.08$ and $\Gamma = 0.01$. In the solar wind region and over a wide range of heliospheric distances, the quantity $|\delta B_{y0}|/B_0$ tends to be small ($\approx 5\%$) (Matthaeus & Goldstein 1982; Roberts *et al.* 1987). The observed filamentary structures of Fig. 1 have a characteristic scale size of the order of the ion gyroradius ρ_s.

4. Discussion and conclusion

We have investigated the transient filamentation instabilities of large-amplitude, KAWs propagating along the background magnetic field. These filaments may act as the source for parametric instabilities of the Alfvén waves and may act as a source of decay waves as well as a source of further collapse. The transverse collapse (filamentation) of KAW produces small scale generation which allows dissipation processes like ion-cyclotron resonance or Laundau damping to act, leading to the heating of the plasma. Self-consistent models can be developed based on the kinetic theory to estimate the plasma heating. The wave number spectrum can be used to estimate the additional heating by calculating the velocity space diffusion coefficient in Fokker-Planck equation.

Acknowledgement

This work was supported by Department of Science & Technology, India.

References

Bellan, P. M., Stasiewicz, K. 1998, *Phys. Rev. Lett.*, **80**, 3523.
Champeaux, S., Passot, T., Sulem, P. L. 1997, *J. Plasma Phys.*, **58**, 665.
Champeaux, S., Passot, T., Sulem, P. L. 1998, *Phys. Plasmas*, **5**, 100.
Goldstein, M. L., Roberts, D. A., Deane, A. E., Ghosh, S., Wong, H. K. 1999, *J. Geophys. Res.*, **104(A7)**, 14,437.
Laveder, D., Passot, T., Sulem, P. L. 2001, *Physica D*, **152–153**, 694.
Laveder, D., Passot, T., Sulem, P. L. 2002, *Phys. Plasmas*, **9**, 293.
Matthaeus, W. H., Goldstein, M. L. 1982, *J. Geophys. Res.*, **87**, 6011.
Roberts, D. A., Klein, L. W., Goldstein, M. L., Matthaeus, W. H. 1987, *J. Geophys. Res.*, **92**, 11,021.
Shukla, A., Sharma, R. P. 2002, *J. Geophys. Res.*, **107(A11)**, 1338, doi: 10.1029/2001JA009135.
Shukla, P. K., Stenflo, L. 1999, *Phys. Plasmas*, **6**, 4120.
Shukla, P. K., Stenflo, L., Bingham, R. 1999, *Phys. Plasmas*, **6**, 1677.
Shukla, P. K., Stenflo, L. 2000, *Phys. Plasmas*, **7**, 2738.